Ag, Al, Ga 对 Sn—9Zn 无铅钎料润湿性能的影响

王 慧, 薛松柏, 陈文学, 王俭辛*
(南京航空航天大学 材料科学与技术学院, 南京 210016)

摘 要: 采用润湿平衡法测试了 Sn—9Zn—X(X 为 Ag, Al, Ga)无铅钎料分别配合 $ZnCl_2$—NH_4Cl 钎剂和免清洗助焊剂, 在空气和氮气保护的两种条件下的润湿性能, 分析研究了合金元素 Ag, Al, Ga 的添加量对 Sn—9Zn—X 无铅钎料润湿性的影响规律。结果表明, 合金元素 Ag, Al, Ga 在 Sn—9Zn 中的最佳添加量(质量分数)分别为 0.3%, 0.005%~0.02%, 0.5%。采用氮气保护可以显著改善 Sn—9Zn—X 无铅钎料的润湿性, 而 Sn—9Zn—X 无铅钎料配合 $ZnCl_2$—NH_4Cl 钎剂时具有较好的润湿性, 甚至优于 Sn—3.5Ag—0.5Cu 在相同条件下的润湿性。这一研究结果表明, 通过研发适合于 Sn—Zn 系无铅钎料的高性能助焊剂, 从而改善 Sn—Zn 系钎料的润湿性能是完全可行的。

关键词: 无铅钎料; Sn—Zn; 合金元素; 润湿性
中图分类号: TG425 文献标识码: A 文章编号: 0253—360X(2007)08—033—05

王 慧

0 序 言

欧盟 WEEE 和 RoHS 指令从 2006 年 7 月 1 日起正式生效, 中国信息产业部等七部委颁布的《电子信息产品污染控制管理办法》于 2007 年 3 月 1 日正式开始实施, 意味着中国以及世界电子行业的"无铅化"制造已经全面启动。

钎料的无铅化是整个"无铅化"进程的关键所在。近年来, 世界各国相继开发出了多种无铅合金体系并已得到广泛应用, 但是, Sn—Zn 系无铅钎料却由于 Zn 的存在, 使得 Sn—Zn 系钎料普遍存在润湿性差、抗氧化性能差、抗腐蚀性能差等缺点, 成为制约 Sn—Zn 合金钎料在电子行业中应用的最大障碍。然而, 不可忽视的是, Sn—Zn 系无铅钎料原材料来源广泛、价格成本低、熔点与 Sn—Pb 共晶钎料相近, 这意味着对于现有的生产设备无需做多大调整就可以实现无铅化生产, 而且共晶 Sn—Zn 无铅钎料具有比 Sn—Pb 钎料更高的焊点抗剪强度, 室温下具有比 Sn—Pb 更好的抗疲劳性能, 电迁移效应也优于 Sn—Pb 钎料[1], 因此, 仍然受到人们的关注。

在 Sn—Zn 合金中添加 Ag, Al, Ga 等合金元素可以改善其润湿性能[2—5], 但是对于合金元素对 Sn—Zn 无铅钎料润湿性的影响规律缺乏系统而深入的研究。作者采用润湿平衡法, 研究了在空气和氮气两种气氛条件下, 配合 $ZnCl_2$—NH_4Cl 钎剂、免清洗助焊剂两种活性不同的助焊剂, Ag, Al, Ga 等合金元素对 Sn—9Zn—X 无铅钎料润湿性能的的影响规律, 研究结果对于推进 Sn—Zn 合金钎料在电子行业中的应用具有重要意义。

1 试验条件

1.1 试验材料与设备

(1) 以 Sn—9Zn 为无铅钎料基材, 分别添加不同含量的合金元素 Ag, Al, Ga, 制备出 12 种不同成分的无铅钎料合金, 元素添加量见表 1。

表 1 Sn—9Zn 中合金元素的添加量(质量分数, %)
Table 1 Addictive element content in Sn-9Zn

Ag	Al	Ga
1.00	0.100	3.00
0.50	0.020	1.00
0.30	0.005	0.50
0.10	0.002	0.10

(2) 标准无氧铜试片, 规格为 0.3 mm×5 mm×30 mm。

(3) $ZnCl_2$—NH_4Cl 钎剂, 免清洗助焊剂。

(4) SAT—5100 型可焊性测试仪(日本 Rhesca 公司)。

(5) 纯度为 99.99%的氮气, 氮气流量 5 L/min,

收稿日期: 2007—04—29
基金项目: 2006 年江苏省"六大人才高峰"资助项目(06—E—020)
*参加此工作的还有韩宗杰

由 LZB—6WB 转子流量计控制。

1.2 试验原理及方法

试验过程参照日本工业标准 JIS Z 3198—4《无铅钎料试验方法—第四部分：基于润湿平衡及接触角法的润湿性试验方法》[6] 进行，将处理完毕待用的试验铜片浸入助焊剂中 5 s 后，立即固定在测试仪的夹具上，用刮刀刮去熔融钎料表面的氧化膜，将铜片以 4 mm/s 的速度垂直浸入熔融钎料中，浸入深度为 2 mm，保持 10 s 后将铜片移出钎料，铜片从浸入熔融钎料的瞬间开始，通过仪器的高性能电子天平来测定试件所受作用力随时间变化的润湿曲线，如图 1 所示。

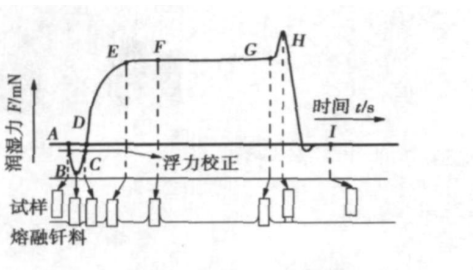

图 1 润湿平衡法的润湿曲线

Fig. 1 Profile of wetting balance method

铜片刚浸入熔融钎料时润湿还没有发生，此时铜片受到的力主要受到负的润湿力和浮力作用，而使曲线向下出现负值，随后铜片开始被润湿，钎料与铜片的接触角不断减小，钎料熔体在铜片上“爬升”，在 D 点润湿力克服浮力，合力为零，此后，随着润湿过程的逐渐进行，合力在 F 点达到最大值。将设备所测到的最大合力加上铜片受到的浮力即得到熔体对铜片的最大润湿力。通过润湿时间和最大润湿力两个参数可对钎料在基板上的润湿性进行评价，润湿时间 t_0 为 A 和 D 之间的时间，最大润湿力为 F 点对应的合力加上钎料熔体对铜片的浮力。润湿时间越短，最大润湿力越大则表明润湿性越好。

试验采用 $ZnCl_2$—NH_4Cl 钎剂和免清洗助焊剂，分别在空气和氮气保护下测量各成分钎料在 245 ℃下的润湿性，同种条件选取重复性较好 5 个数据取平均值，通过润湿时间和润湿力评价钎料在铜基板上的润湿性能。

2 试验结果及分析

2.1 Ag 添加量对 Sn—9Zn 润湿性的影响

图 2 为不同 Ag 含量的 Sn—9Zn—xAg 钎料在不同试验条件下，润湿时间和润湿力的比较。从图 2a 可知，Ag 元素含量在 0.3%以下时，钎料在铜板上的润湿时间随 Ag 元素含量升高而减小，当 Ag 元素含量继续上升到 0.5%时，润湿时间反而增大，在使用免清洗助焊剂的条件下，润湿时间已大于 Sn—9Zn 在相同条件下的润湿时间。图 2b 为不同 Ag 含量 Sn—9Zn—xAg 润湿力的比较，与图 2a 相对应，当 Ag 元素含量在 0.3%时合金在铜基板上的润湿力较大，说明在 Sn—9Zn 中添加 0.3%的 Ag 时，钎料的润湿性改善最为明显，但是当 Ag 元素的含量大于 0.5%时，钎料中会形成颗粒状的 Ag_5Zn_8，$AgZn_3$[7] 金属间化合物，这种金属间化合物的存在降低液态钎料的流动性，阻碍了液态钎料在铜基板上的“爬升”，而且 Ag 含量越高，钎料的熔点随之增高，从而导致 Ag 含量过高，反而会使钎料的润湿性能恶化。此外，使用 $ZnCl_2$—NH_4Cl 钎剂时，Sn—9Zn—xAg 的润湿性能明显要优于使用免清洗助焊剂时的润湿性能；在同种助焊剂的条件下，使用氮气保护可以明显改善 Sn—9Zn—xAg 的润湿性能，其原因可能是一方面在氮气气氛下钎料熔体的表面张力减小[8]，另一方面氮气保护减少了表面 Zn 的氧化。

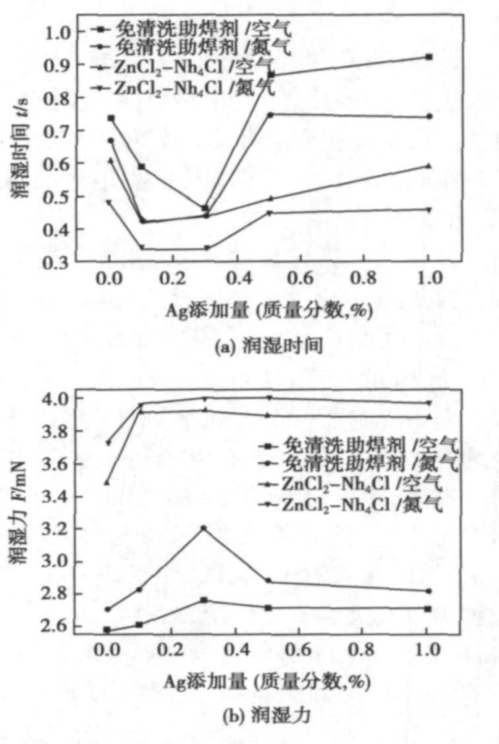

图 2 245 ℃时 Sn—9Zn—xAg 的润湿时间及润湿力

Fig. 2 Wetting time and wetting force of Sn-9Zn-xAg at 245 ℃

2.2 Al 添加量对 Sn—9Zn 润湿性的影响

图 3 为不同 Al 含量的 Sn—9Zn—xAl 钎料在不

同试验条件下，润湿时间和润湿力的比较。由图 3a 可知，在使用免清洗助焊剂的条件下，Al 元素含量在0.005%时润湿时间最小，当 Al 元素含量为 0.02%时，润湿时间反而大于 Sn－9Zn 在相同条件下的水平，当 Al 元素含量为 0.1%时，钎料已经不能在铜板上润湿；从图 3b 中也可以看出，在使用免清洗助焊剂的条件下，Al 元素含量在 0.005%时，钎料在铜基板上的润湿力最大。这是因为少量 Al 添加到钎料中，Al 在液态钎料表面形成致密的氧化铝膜改变了液态钎料表面的氧化膜结构，一定程度上阻碍了氧与钎料中 Zn 的接触，减少了 Zn 的氧化，从而改善了钎料的润湿性能[9]；但是当 Al 元素含量大于 0.005%时，在钎料表面形成的氧化铝膜较厚，过厚的氧化膜虽然能够减少 Zn 的氧化，但同时其本身也会使钎料的润湿性能恶化。而在使用 $ZnCl_2$—NH_4Cl 钎剂时，由于其活性较强，Al 添加量在 0.02%时获得最好的润湿性能。

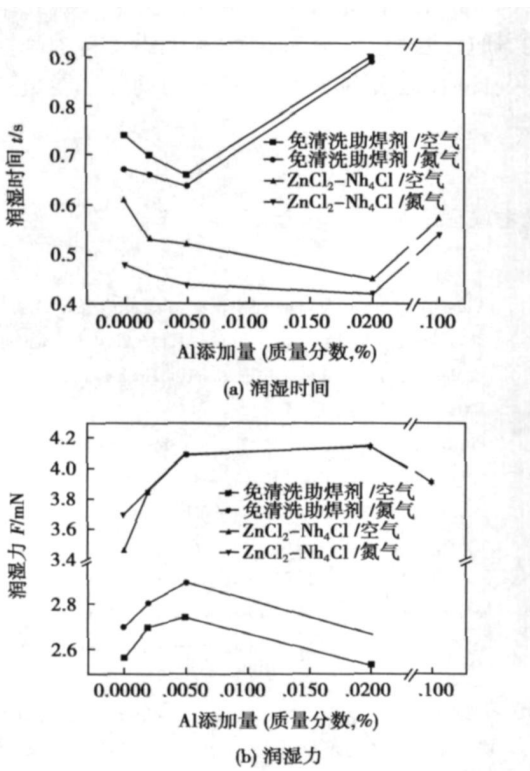

图 3　245 ℃时 Sn—9Zn—xAl 的润湿时间及润湿力

Fig. 3　Wetting time and wetting force of Sn-9Zn-xAl at 245 ℃

2.3　Ga 添加量对 Sn—9Zn 润湿性的影响

图 4 为不同 Ga 含量的 Sn—9Zn—xGa 钎料在不同试验条件下，润湿时间和润湿力的比较。如图 4a 所示，随着 Ga 添加量的增加，钎料在铜板上的润湿时间不断降低，当 Ga 元素含量为 0.5%时，润湿时间已有明显降低，随着 Ga 含量的继续增加，润湿时间变化不大，从图 4b 中可以看出，当 Ga 元素含量在 1%时，钎料在铜基板上的润湿力达到最大值，之后趋于稳定。Ga 的熔点只有 29.8 ℃，添加 Ga 以后，合金的熔点会下降[10]；另外 Ga 又是表面活性元素，添加以后会在液态合金表面富集，富集的结果改变了液态合金表面的组成和结构，减少了 Zn 的氧化，从而改善了钎料的润湿性。早期的研究证明，微量 Ga 添加到 Sn—Pb 钎料中后，会在表层 70～100 Å 处富集34 000 倍之多，形成致密的保护膜[11]，文中所使用的 Sn—9Zn 合金亦和 Sn—Pb 钎料添加微量 Ga 以后的变化相似，但是 Ga 的添加量却有显著的差别，比在 Sn—Pb 钎料中的添加量高出了 100 倍以上。当 Ga 元素含量超过 1%时，表面上 Ga 的浓度富集才达到稳定，液态钎料的润湿性能也趋于稳定，不再变化。

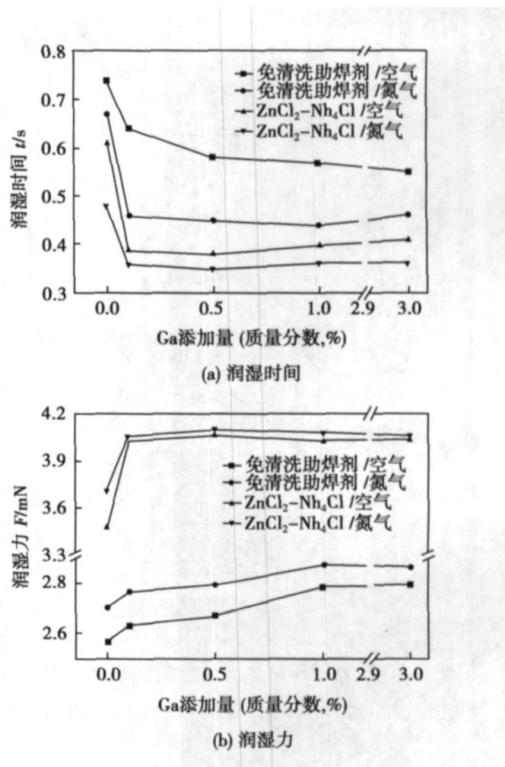

图 4　245 ℃时 Sn—9Zn—xGa 的润湿时间及润湿力

Fig. 4　Wetting time and wetting force of Sn-9Zn-xGa at 245 ℃

2.4　不同成分的合金润湿性比较

图 5 为 Sn—9Zn，Sn—9Zn—0.005Al，Sn—9Zn—0.5Ga，Sn—9Zn—0.3Ag，Sn—3.5Ag—0.5Cu（图 5 中分别用 a，b，c，d，e 表示）在 245 ℃下润湿时间与润湿力的比较，从图 5a 可知，添加 0.3% Ag，0.005% Al，0.5%Ga 后，钎料在铜基板上的润湿时间相比 Sn

－9Zn 明显减小，润湿力也有所提高，钎料的润湿性得到改善。另外，从图中还可以看出，Sn－Zn 钎料在使用 $ZnCl_2$－NH_4Cl 钎剂条件下比使用免清洗助焊剂时表现出更好的润湿性，甚至超过了 Sn－3.5Ag－0.5Cu 在相同条件下的润湿性，这说明试验采用的免清洗助焊剂主要是针对 Sn－Ag－Cu 系无铅钎料而设计的，对于 Sn－Zn 系钎料的助焊效果并不理想，这也是目前市面上出售的免清洗助焊剂普遍存在的问题。这一研究结果表明，通过研发适合于 Sn－Zn 系无铅钎料的高性能助焊剂，从而改善 Sn－Zn 系钎料的润湿性能是完全可行的。

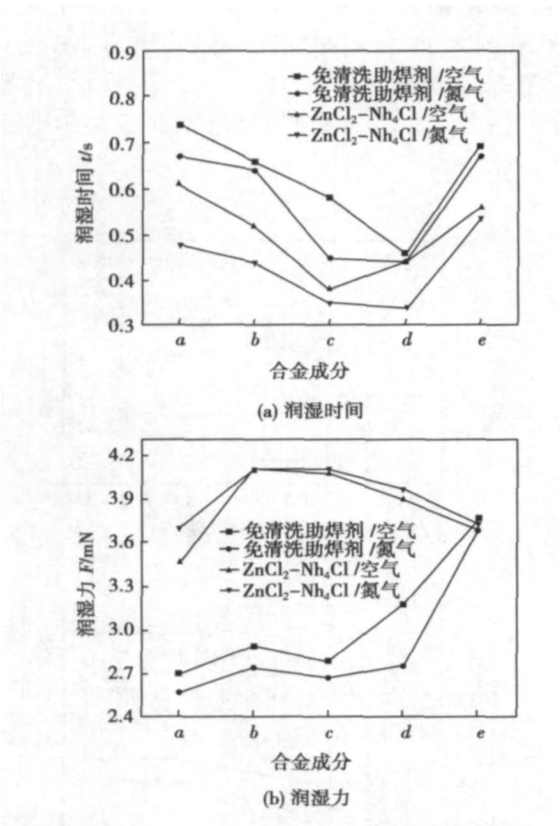

图 5 245 ℃下不同成分合金的润湿时间及润湿力

Fig. 5 Wetting time and wetting force of different alloys at 245 ℃

3 结 论

（1）在 Sn－9Zn 中添加少量 Ag 可以改善其润湿性能，Ag 的添加量在 0.3%最佳；当 Sn－9Zn－xAg 中 Ag 元素含量高于 0.5%时，液态钎料中形成的颗粒状 Ag_5Zn_8，$AgZn_3$ 金属间化合物，降低了液态钎料的流动性，反而会使其润湿性能恶化。

（2）在 Sn－9Zn 中添加微量 Al 后，Al 在液态钎料表面形成的氧化铝膜改变了液态钎料表面的氧化膜结构，一定程度上阻碍了氧与钎料中 Zn 的接触，减少了 Zn 的氧化，从而改善了钎料的润湿性能；但 Al 的添加量过多，表面形成的氧化膜过厚，也会恶化钎料的润湿性能，在使用免清洗助焊剂时，Al 的最佳添加量在 0.005%左右，而在使用 $ZnCl_2$－NH_4Cl 钎剂时 Al 的最佳添加量在 0.02%左右。

（3）少量 Ga 添加到 Sn－9Zn 中后，合金的熔点会降低。由于 Ga 是表面活性元素，添加以后会在合金的表面富集，改变了液态合金表面的组成和结构，减少了 Zn 的氧化，从而改善了钎料的润湿性。当 Ga 元素含量超过 1%时，液态合金表面上 Ga 的浓度不再显著上升，钎料的润湿性趋于稳定。

（4）采用氮气保护可以降低液态钎料的表面张力，而且能够减少液态钎料表面 Zn 的氧化，改善 Sn－Zn－X 钎料的润湿性能。Sn－Zn－X 无铅钎料在使用 $ZnCl_2$－NH_4Cl 钎剂条件下比使用免清洗助焊剂时表现出更好的润湿性，甚至超过了 Sn－3.5Ag－0.5Cu 在相同条件下的润湿性。这一研究结果表明，通过研发适合于 Sn－Zn 系无铅钎料的高性能助焊剂，从而改善 Sn－Zn 系钎料的润湿性能是完全可行的。

参考文献：

[1] Villain I, Jillek W, Schmitt E, *et al*. Properties and reliability of Sn－Zn－Based lead-free solder alloys[C] // 2004 International IEEE Conference on Asian Green Electronics. Hong Kong, China, IEEE, 2004.

[2] Lin K L, Chen K I, Hsu H M, *et al*. Improvement in the properties of Sn－Zn eutectic based Pb-free solder[C] // 53rd Electronic Components and Technology Conference. New Orleans, Louisiana, IEEE, 2003.

[3] Nai S L, Lin K L. The effect of Ga content on the wetting reaction and interfacial morphology formed between Sn-8.55Zn-0.5Ag-0.1Al-xGa solders and Cu[J]. Scripta Materialia, 2006, 54(2): 219－224.

[4] Chen K I, Cheng S C, Wu S, *et al*. Effects of small additions of Ag, Al, and Ga on the structure and properties of the Sn－9Zn eutectic alloy[J]. Journal of Alloys and Compounds, 2006, 416(1－2): 98－105.

[5] 黄惠珍，黄起森，彭 曙，等. 添加 Ag 对 Sn9Zn 无铅钎料合金性能的影响[J]. 特种铸造及有色合金，2006，26(3)：179－181.

[6] 王春青，李明雨，田艳红，等. JIS Z 3198 无铅钎料试验方法简介与评述[J]. 电子工艺技术，2004，25(3)：50－54.

[7] Tsai Y L, Hwang W S. Solidification behavior of Sn-9Zn-xAg lead-free solder alloys[J]. Materials Science and Engineering, 2005, A413－A414: 312－316.

[下转第 44 页]

luminium alloys[J]. Materials Science and Engineering A, 2003, 363(1—2): 40—52.

[5] Palanco S, Klassen M, Skupin J, *et al*. Spectroscopic diagnostics on CW—laser welding plasmas of aluminum alloys[C] // 1st International Conference on Laser Induced Plasma Spectroscopy and Applications. Elsevier Science B V, 2001: 651—659.

[6] 赵熹华, 曹海鹏, 赵 贺. 激光束—电阻缝焊复合焊接方法基础研究[C] // 第十一次全国焊接会议论文集. 哈尔滨: 黑龙江人民出版社, 2005: 388—390.

[7] 杜汉斌, 胡伦骥, 王东川. 激光穿透焊温度场及流动场的数值模拟[J]. 焊接学报, 2005, 26(12): 65—68.

作者简介: 熊智军, 男, 1981 年出生, 硕士研究生。主要研究方向为焊接方法与机电一体化。

Email: bearxzj_yuan@sina.com

[上接第 36 页]

[8] 刘汉城, 汪正平, 李宁成, 等. 电子制造技术[M]. 姜岩峰, 张常年, 译. 北京: 化学工业出版社, 2005.

[9] Kitajima M, Shono T. Development of Sn—Zn—Al lead-free solder alloys[J]. Fujitsu Scientific and Technical Journal, 2005, 41(2): 225—235.

[10] Zhang Yue, Liang Tongxiang, Jusheng M A. Phase diagram calculation on Sn—Zn—Ga solders[J]. Journal of Non-Crystalline Solids, 2004, 336(2): 153—156.

[11] 张启运, 刘淑琪, 刘东升, 等. 微量添加元素对熔态 Sn—Pb 共晶合金抗氧化能力的影响[J]. 金属学报, 1984, 20(4): A296—A302.

作者简介: 王 慧, 男, 1982 年出生, 博士研究生。主要从事微电子焊接技术及无铅钎料研究工作。发表论文 2 篇。

Email: huiwang@nuaa.edu.cn

vanced Materials Processing Technology, Ministry of Education, Beijing 100084, China). p17—20

Abstract: The embedded Real Time Operating System (RTOS) and Micro Controller Operating System-Ⅱ (μC/OS-Ⅱ) are successfully transplanted and applied in the digital-controlled inverter arc welding power supply, which based on the dual Digital Signal Processors. For numerous affairs during welding process, after the assignment of multitasks with clear functions, scheduling of multitasks and supervising of multi-states are carried out, and the supervising on the working states of power supply in real time, and the fast and correct judgment and protection action on the faults of power supply, such as the faults of input/output model, the faults of inverter model and the faults of welding assistant equipment etc., are achieved, which guarantees the working reliability and security of welding power supply. Moreover, through the harmony and cooperation of multitasks, the friendly alternation between various working states and users are realized in real time, thus the accuracy of faults identification on power supply system and its maneuverability are improved, and the problems of digital management of real-time states of inverter arc welding power supply and digital comprehensive management of the whole welding machine are solved.

Key words: supervising and management in real time; digital-controlled inverter arc welding power supply; real time operating system; multitasks system

Cutting picker with high chromium Fe-based composite coating prepared by plasma surface metallurgy LIU Junbo (School of Mechanical and Electronic Engineering, Weifang University, Weifang 261061, Shandong, China). p21—24

Abstract: The high chromium Fe-based composite coating was successfully fabricated on the low-carbon low alloy steel by plasma surface metallurgy with the powders which were obtained by heating a mixture powders and sucrose to pyrolyze the sucrose as carbonaceous precursor. The microstructure and microhardness of the coating were studied by scanning electron microscope, X-ray diffraction, energy dispersion spectroscope and microhardness instrument. Wear and impact test were also analyzed by wear tester and impact tester. The results indicate that the interface between coating and matrix of the composite was metallurgically bonded, and the matching performance of the coating was excellent and each performance advantages were developed. The composite was used to coat cutting picker, which simplify the heat-treatment process and reduce the production costs. It indicate that all of the properties surpassed the industry technical standards.

Key words: precursor; reactive plasma surface metallurgy; composite coating; cutting picks

Preparation of TiB_2+ Ni/Ni_3Al/ stainless steel gradient material via FASHS SHEN Yanli[1], MENG Qingsen[1], Z. A. Munir[2], XIN Lijun[1], HU Lifang[1] (1. School of Material Science and Engineering, Taiyuan University of Technology, Taiyuan 030024, China; 2. School of Chemical Engineering and Materials Science, University of California, Davis, USA). p25—28, 32

Abstract: TiB_2+ Ni/Ni_3Al/stainless steel gradient material was prepared by mechanical alloying and field-activated self-propagating high-temperature synthesis (FASHS). At first, in order to stimulate the combustion reaction, Ni powder and Al powder were mechanical alloying, then TiB_2+ Ni/Ni_3Al/405 stainless steel gradient material was prepared by the reaction thermal of self-propagating combustion reaction. The interface, the microstructure and the phase composition of the gradient material were observed by scanning electron microscope and X-ray diffraction, and metallurgical bonding layer was formed in the interfaces of cermet, Ni_3Al, 405 stainless steel. The mechanical properties, the hardness and the resistance to wear of gradient material were studied by Rockwell hardometer, microhardness tester and grinding abrasion tester; and the results show that cermet surface Rockwell hardness is 90 HRA, and the chemical constitution and the microhardness of material were gradient and the resistance to wear exceed 20Cr case-hardened stell.

Key words: self-propagating high-temperature synthesis; gradient material; cermet; joining

Microstructure of interface between Ag—Cu—Ti brazing filler metal and diamond LU Jinbin[1,2], XU Jiuhua[2] (1. School of Materials and Chemical Engineering, Zhongyuan University of Technology, Zhengzhou 450007, China; 2. Nanjing University of Aeronautics and Astronautics, Nanjing 210016, Chian). p29—32

Abstract: The high-strength bonding between steel matrix and diamond grit was obtained by using Ag—Cu—Ti brazing filler metal in vacuum furnace. The microstructure on the interface between diamond and the filler metal and carbide which was formed on the diamond surface was observed with scanning electron microscope, and the change of components in it was analyzed with energy dispersion spectroscope and the structure of the diamond was analyzed with Raman. Results showed that Ti in Ag—Cu—Ti separated out at the interface to form lump-like TiC carbide on the surface of diamond, which was less than 1 μm in size. Meanwhile, the diamond wasn't graphitized in the high temperature. As a result, the serial of diamond-TiC-filler metal-steel matrix was formed between the interface of the diamond and the filler metal.

Key words: brazing; TiC; diamond

Effect of Ag, Al, Ga addition on wettability of Sn-9Zn lead-free solder WANG Hui, XUE Songbai, CHEN Wenxue, WANG Jianxin (College of Materials Science and Technology, Nanjing University of Aeronautics and Astronautics, Nanjing 210016, China). p33—36, 44

Abstract: Wettability of Sn—9Zn—X (Ag, Al, Ga) lead-free solder, with non-cleaning flux and $ZnCl_2$—NH_4Cl flux, was appraised by means of wetting balance method in air and N_2 atmospheres; the effect of different additive amount of Ag, Al, Ga on the wettability of Sn—9Zn—X solders was studied. The results indicate that the optimum additive amount of Ag, Al, Ga in Sn—9Zn solder is 0.3, 0.005—0.02 and 0.5 mass percent, respectively. The wet-

tability of Sn—9Zn—X can be obviously improved in N_2 atmospheres. It is also found that Sn—9Zn—X lead-free solders show preferable wettability with $ZnCl_2$—NH_4Cl flux, even better than that of Sn—3.5Ag—0.5Cu solder under the same condition, which may reveal the feasibility of improving the wettability of Sn—Zn series lead-free solders by developing suitable flux.

Key words: lead-free solder; Sn—Zn solder; alloy element; wettability

Welding characteristics of laser-low power pulse MIG hybrid welding aluminium alloy WANG Wei, WANG XuYou, QI GuoLiang, LEI Zhen, LIN ShangYang, DU Bing (Harbin Welding Institute, Harbin 150080, China). p37—40, 61

Abstract: The weld penetration, formation of weld, welding speed and weld heat input of MIG (metal inert-gas) welding and laser-MIG hybrid welding are analyzed for welding 5A06 aluminum alloy. It is shown that comparing with MIG welding, laser-MIG hybrid welding will increase depth-to-width ratio 100%—200% and increase weld penetration 43%—250%, as average current is less than 200 A and welding heat input and welding speed are equal. If welding heat input and average welding current are equal, welding speed of laser-MIG hybrid welding is higher 0.6—1.5 times than that of MIG welding, and weld penetration of laser-MIG hybrid welding is deeper 1.5—6.9 times than that of MIG welding. Equal weld penetration of laser-MIG hybrid welding and MIG welding can be obtained if lower welding heat input is applied in the hybrid welding and welding speed of the hybrid welding is 0.6—6.5 times higher than the one of MIG welding. Laser-MIG hybrid welding has good weld spreadability and is fit for high speed welding. It also was found that 2 kW laser power compounding with MIG will increase average arc voltage and decrease average welding current of MIG welding.

Key words: hybrid welding; laser welding; MIG welding; aluminum alloy welding

Numerical simulation of temperature field in deep penetration laser welding under hot and press condition XIONG Zhijun, LI Yongqiang, ZHAO Xihua, LI Min, ZHANG Weihua (School of Materials Science and Engineering, Jilin University, Changchun 130022, China). p41—44

Abstract: Deep penetration laser welding was performed at aluminum alloy LF3Y2 under hot and press condition. A heat source model, which comprises a gauss plane heat source on the top surface and a revolved gauss body heat source, was presented in this condition. Numerical simulation was adopted by the heat source model and ANSYS software. The results show that sufficient width and penetration of weld could be obtained under high speed welding operation and the isotherms looked like ellipse. The temperature gradient was correspondingly higher in the front of moving heat source than at the end. The cross-section morphology of simulation welded joint was almost in accordance with the results attained by experiments which confirmed the reasonableness of the model.

Key words: deep penetration laser welding; heat source model; numerical simulation; temperature field

Effect of magnetic field on microstructure and properties of carbon arc surfacing layer LIU Zhengjun, ZHANG Guiqing, YIN Yijun, ZENG Xiebo (School of Material Science and Engineering, Shenyang University of Technology, Shenyang 110023, China). p45—48

Abstract: In order to refine the structure of deposited metal and control the morphology and distribution of hard phases in surfacing deposited metal, DC transverse magnetic field was applied to the carbon arc surfacing of Cr—B—Ni—V iron based alloy system. The influence of magnetic intensity on hardness and wearing resistance was obtained through analyzing the hardness, wearing and microstructures of the surfacing deposited metal. The results show that the surfacing deposited metal of introducing magnetic field has higher hardness and better wearing resistance than the surfacing deposited metal without magnetic field; the properties of surfacing deposited metal are optimal when magnetic field current is 3 A, and surfacing current is 180 A, and surfacing speed is 12 cm/min. The hard phase in the surfacing deposited metal is fine and even, hexagonal in shape. Mean while the orientation of them is consistent.

Key words: transverse magnetic field; hardfacing; grinding abrasion; hard phase

Mechanical properties of ring nugget in sheet-to-tube joining LIANG Caiping, ZHANG Yansong, LAI Xinmin, CHEN Guanlong (School of Mechanical Engineering, Shanghai Jiao tong University, Shanghai 200030, China). p49—53

Abstract: Strength of resistance spot weld is determined by the physical attributes of weldment including material and geometric issues. The strength of the ring nugget in sheet-to-tube single-sided spot welding is different from that of the button nugget in traditional sheet-to-sheet spot welding. And the relationships between strength and attributes of ring nugget are unknown. Meanwhile, the large number of variables and experimental uncertainty also make it difficult to establish this relationships. A numerical simulation experiment was conducted using the concept of design of experiments (DOE) and the method of finite element based on the tensile-shear tests. The mechanical properties during tensile-shear process was analyzed and quantitative relationships were established to link a weld's tensile-shear force and its geometrical attributes, which supplied the proof for the nugget quality estimation.

Key words: single-sided spot welding; numerical simulation; ring nugget; mechanical properties

Extraction of welding pool shape using linear approximation WANG Jifeng, WANG Wenyi, CHEN Shanben (Institute. of Welding Technology, Shanghai Jiaotong University, Shanghai 200030, China). p54—56

Abstract: The welding bead shape is crucial for welding quality. Three-dimensional shape of the welding pool contain much information about quality. Thus, shape from shading technique was